

## ARTICLE OPEN



# A novel function of STAT3 $\beta$ in suppressing interferon response improves outcome in acute myeloid leukemia

Sophie Edtmayer<sup>1</sup>, Agnieszka Witalisz-Siepracka<sup>1</sup>, Bernhard Zdársky<sup>1</sup>, Kerstin Heindl<sup>1</sup>, Stefanie Weiss<sup>1</sup>, Thomas Eder<sup>2</sup>, Sayantane Dutta<sup>3</sup>, Uwe Graichen<sup>4</sup>, Sascha Klee<sup>4</sup>, Omar Sharif<sup>5,6</sup>, Rotraud Wieser<sup>7,8</sup>, Balázs Gyórfy<sup>9,10,11</sup>, Valeria Poli<sup>12</sup>, Emilio Casanova<sup>13</sup>, Heinz Sill<sup>14</sup>, Florian Grebien<sup>15</sup> and Dagmar Stoiber<sup>16</sup>✉

© The Author(s) 2024

Signal transducer and activator of transcription 3 (STAT3) is frequently overexpressed in patients with acute myeloid leukemia (AML). STAT3 exists in two distinct alternatively spliced isoforms, the full-length isoform STAT3 $\alpha$  and the C-terminally truncated isoform STAT3 $\beta$ . While STAT3 $\alpha$  is predominantly described as an oncogenic driver, STAT3 $\beta$  has been suggested to act as a tumor suppressor. To elucidate the role of STAT3 $\beta$  in AML, we established a mouse model of STAT3 $\beta$ -deficient, *MLL-AF9*-driven AML. STAT3 $\beta$  deficiency significantly shortened survival of leukemic mice confirming its role as a tumor suppressor. Furthermore, RNA sequencing revealed enhanced STAT1 expression and interferon (IFN) signaling upon loss of STAT3 $\beta$ . Accordingly, STAT3 $\beta$ -deficient leukemia cells displayed enhanced sensitivity to blockade of IFN signaling through both an IFNAR1 blocking antibody and the JAK1/2 inhibitor Ruxolitinib. Analysis of human AML patient samples confirmed that elevated expression of IFN-inducible genes correlated with poor overall survival and low STAT3 $\beta$  expression. Together, our data corroborate the tumor suppressive role of STAT3 $\beta$  in a mouse model in vivo. Moreover, they provide evidence that its tumor suppressive function is linked to repression of the STAT1-mediated IFN response. These findings suggest that the STAT3 $\beta$ /*a* mRNA ratio is a significant prognostic marker in AML and holds crucial information for targeted treatment approaches. Patients displaying a low STAT3 $\beta$ /*a* mRNA ratio and unfavorable prognosis could benefit from therapeutic interventions directed at STAT1/IFN signaling.

*Cell Death and Disease* (2024)15:369; <https://doi.org/10.1038/s41419-024-06749-9>

## INTRODUCTION

Acute myeloid leukemia (AML) is an aggressive form of leukemia occurring both in children and adults. The development of effective therapeutic strategies is complex due to the wide array of cytogenetic and molecular abnormalities observed in patients. Although targeted therapies with small molecule inhibitors of FLT3, BCL2, and IDH1/2 have improved disease outcomes for several AML subtypes, the 5-year survival rate remains only around 30% [1]. Thus, novel treatment combinations and prognostic markers are urgently needed.

Signal transducer and activator of transcription 3 (STAT3) is an important transcription factor regulating stem cell self-renewal, hematopoiesis, and inflammation [2]. Aberrant STAT3 signaling promotes proliferation and survival in various malignancies and therefore has been explored as a therapeutic target [3]. Moreover, enhanced STAT3 activity is associated with poor prognosis and

increased resistance to chemotherapy [4–8]. In AML, constitutive STAT3 activation was reported in AML patient samples and cell lines and contributes to leukemia cell survival, uncontrolled proliferation, and evasion of apoptosis [4, 6–9]. Importantly, alternative splicing gives rise to two isoforms with distinct functions contributing to the diverse roles of STAT3 in cancer [10–12]. While STAT3 $\alpha$  represents the full-length isoform, STAT3 $\beta$  is truncated due to an alternative acceptor site causing a C-terminal deletion of 55 amino acids. Consequently, STAT3 $\beta$  lacks the transactivation domain including the phosphorylation site serine 727 [13]. Therefore, STAT3 $\beta$  was initially considered as a negative regulator of STAT3 $\alpha$  [14]. However, studies demonstrated that STAT3 $\beta$  plays a relevant role as a transcriptional regulator as it was capable of rescuing the embryonic lethality in STAT3 $\alpha$ -deficient mice [11, 12]. Furthermore, STAT3 $\beta$  was reported to induce transcription of a distinct set of genes in a STAT3 $\alpha$ -

<sup>1</sup>Division Pharmacology, Department of Pharmacology, Physiology and Microbiology, Karl Landsteiner University of Health Sciences, Krems, Austria. <sup>2</sup>Institute for Medical Biochemistry, University of Veterinary Medicine Vienna, Vienna, Austria. <sup>3</sup>Division of Oncology, Medical University of Graz, Graz, Austria. <sup>4</sup>Division Biostatistics and Data Science, Department of General Health Studies, Karl Landsteiner University of Health Sciences, Krems, Austria. <sup>5</sup>Institute for Vascular Biology, Centre for Physiology and Pharmacology, Medical University of Vienna, Vienna, Austria. <sup>6</sup>Christian Doppler Laboratory for Immunometabolism and Systems Biology of Obesity-Related Diseases (InSpiReD), Vienna, Austria. <sup>7</sup>Division of Oncology, Department of Medicine I, Medical University of Vienna, Vienna, Austria. <sup>8</sup>Ludwig Boltzmann Institute for Hematology and Oncology, Medical University of Vienna, Vienna, Austria. <sup>9</sup>Department of Bioinformatics, Semmelweis University, Budapest, Hungary. <sup>10</sup>Department of Biophysics, Medical School, University of Pecs, Pecs, Hungary. <sup>11</sup>Cancer Biomarker Research Group, Institute of Molecular Life Sciences, HUN-REN Research Centre for Natural Sciences, Budapest, Hungary. <sup>12</sup>Department of Molecular Biotechnology and Health Sciences, University of Turin, Turin, Italy. <sup>13</sup>Department of Pharmacology, Center of Physiology and Pharmacology & Comprehensive Cancer Center (CCC), Medical University of Vienna, Vienna, Austria. <sup>14</sup>Division of Hematology, Medical University of Graz, Graz, Austria. <sup>15</sup>St. Anna Children's Cancer Research Institute (CCRI), Vienna, Austria. <sup>16</sup>CeMM Research Center for Molecular Medicine of the Austrian Academy of Sciences, Vienna, Austria. ✉email: dagmar.stoiber@kl.ac.at

Edited by Marc Diederich

Received: 14 December 2023 Revised: 8 May 2024 Accepted: 15 May 2024

Published online: 28 May 2024

independent manner [11, 12, 15, 16]. In more recent studies, STAT3β gained attention as a tumor suppressive molecule in melanoma [17], lung cancer [18], and esophageal squamous cell carcinoma [16]. In our previous study, we demonstrated that a higher *STAT3β/α* mRNA ratio correlates with prolonged overall survival (OS) in AML patients [19]. Moreover, overexpression of STAT3β in murine leukemia cells delayed disease progression in mice [19]. However, the molecular mechanisms behind its protective role remained elusive.

Here, we provide insights into the cellular processes resulting in the tumor suppressive function of STAT3β in AML and assign a link between STAT3 isoform expression and interferon (IFN) signaling in leukemia cells. Absence of STAT3β led to an enhanced IFN response and unfavorable disease outcomes, both in an AML mouse model and in primary AML patient samples. Furthermore, STAT3β-deficient leukemia cells were specifically vulnerable to interference with IFN signaling through the JAK1/2 inhibitor Ruxolitinib. Patients with a lower *STAT3β/α* mRNA ratio and unfavorable prognosis might benefit from treatment combinations with Ruxolitinib.

## MATERIALS AND METHODS

Additional methods can be found in Supplementary Materials and Methods.

### AML patients

Diagnostic samples (peripheral blood and bone marrow aspirates) from 79 AML patients were collected after written informed consent at the Medical University of Graz (Austria) and processed as described [20]. Only patients receiving curative treatment were included [21]. Patients with FLT3 aberrations, associated with elevated STAT5 signaling, were excluded [22–26]. For patient characteristics see Supplementary Table 1. Publicly available gene expression data sets were analyzed with Kaplan-Meier Plotter [27] ( $n = 443$ ) and BloodSpot [28] ( $n = 244$ ).

### Animal studies

Mice were kept under pathogen-free conditions at the Institute of Pharmacology, Medical University of Vienna (Austria). STAT3β-deficient mice were generated by Maritano et al. [11]. For the AML model, fetal liver cells were isolated and retrovirally transduced as described [19].  $2 \times 10^5$  Venus<sup>+</sup> cells were transplanted into 6–8 weeks old male immunocompromised NOD.Cg-Prkdc<sup>scid</sup>Il2rg<sup>tm1Wjl</sup>/SzJ mice (The Jackson Laboratory) via tail vein injection.

### Flow cytometry

Unspecific Fc-receptor binding was blocked using an anti-CD16/CD32 antibody (BD Bioscience, Franklin Lakes, NJ, USA). Antibodies (Supplementary Table 3) were added to cell suspension at 1:100–1:200 in PBS containing 2% FBS, incubated for 30 min on ice and protected from light, and afterwards washed twice using PBS. Samples were measured using a Cytoflex S (Beckman Coulter, Brea, California, USA), and data was analyzed with CytExpert (Beckman Coulter) or FlowJo software (TreeStar, Ashland, OR, USA). Living cells were determined according to FSC and SSC and viability was confirmed using 7-AAD staining. Gating was performed using negative controls (untransfected cells or unstained samples) and single-staining controls.

### Colony formation assay

$1 \times 10^4$  cells were seeded in 1 ml methylcellulose with recombinant cytokines (SCF, IL-3, IL-6, and EPO) for mouse cells (MethoCult<sup>TM</sup> GF M3434, Stemcell Technologies, Vancouver, Canada) in 35 mm cell culture dishes and incubated at 37 °C, 95% humidity and 5% CO<sub>2</sub>. After 7 days colonies were counted and harvested for immunophenotyping via flow cytometry. For treatments 2 μg/ml IFNAR1 blocking antibody (clone: MAR1-5A3, BioLegend, San Diego, CA, USA), 2 μg/ml IgG isotype control (Invitrogen, Thermo Fisher Scientific, Waltham, MA, USA), 5 μM Ruxolitinib (LC Laboratories, MA, USA) or 0.05% DMSO (Carl Roth, Mannheim, Germany) was supplemented. All images were obtained after 7 days in methylcellulose using an Olympus CKX53 microscope (Olympus, Tokyo, Japan) and an Olympus EP50 camera.

## Statistics

**Patient data.** Stratification in our cohort and in the Kaplan-Meier Plotter into high and low gene expression was performed according to Nagy et al. [29]. Survival analysis was performed using Kaplan-Meier estimates and log-rank (Mantel-Cox) test.

**Animal and in vitro data.** Survival was analyzed using Kaplan-Meier estimates and log-rank (Mantel-Cox) tests. Other data sets were analyzed with unpaired Student's *t*-test using GraphPad Prism. The Shapiro-Wilk test was carried out to test for normal distribution. Outliers were excluded based on Grubbs' test with significance level  $\alpha = 0.05$ . Error bars represent means  $\pm$  SD from at least three independent biological or technical replicates. *p*-values are indicated as  $p \leq 0.05$ \*,  $\leq 0.01$ \*\*\*,  $\leq 0.001$ \*\*\*\*, and  $\leq 0.0001$ \*\*\*\*. Lack of statistical significance was indicated with "ns".

## RESULTS

### STAT3β-deficient leukemia cells display increased colony formation potential and are less committed to the myeloid lineage

To mimic the characteristics of AML blasts, we used an AML mouse model driven by the *MLL-AF9* fusion oncogene that results from the t(9;11)(p22;q23) translocation, which is found in AML patients and associated with an intermediate prognosis [30–32]. Fetal liver cells (FLCs) were isolated from wildtype (WT) and STAT3β-deficient ( $\Delta\beta$ ) mice and transduced with a retroviral vector encoding *MLL-AF9*, coupled to a Venus fluorescence reporter (Fig. 1A) [11, 33]. The genotype was confirmed via PCR (Supplementary Fig. 1A). A similar expression of STAT3α on the mRNA and protein levels (Supplementary Fig. 1B, Fig. 1B) was observed in established homogenous Venus<sup>+</sup> cells (Supplementary Fig. 1C) that were utilized for all in vitro experiments. Although the absence of STAT3β neither led to a proliferative advantage (Fig. 1C) nor affected cell cycle regulation (Supplementary Fig. 1D) or apoptosis in suspension culture (Supplementary Fig. 1E), STAT3β-deficiency resulted in increased colony formation capacity upon serial replating in methylcellulose (Fig. 1D). Both WT and STAT3β-deficient leukemia cells gave rise to myeloid-type colonies and exhibited similar viability after 7 days (Supplementary Fig. 1F) but displayed a different colony morphology (Fig. 1E, Supplementary Fig. 1G). Immunophenotyping revealed that STAT3β-deficient colonies were comprised of significantly fewer mature myeloid cells, as defined by the myeloid surface markers CD11b and Gr-1, but contained more Sca-1<sup>+</sup> cells (Fig. 1F), while no discernible differences were observed in suspension culture (Supplementary Fig. 1H). In summary, these experiments demonstrate that loss of STAT3β does not accelerate proliferation but enhances colony forming ability of *MLL-AF9*-transformed FLCs. Furthermore, our findings suggest that STAT3β promotes myeloid differentiation of leukemia cells.

### Leukemia cells lacking STAT3β exhibit reduced differentiation response to G-CSF

To explore the function of STAT3β during differentiation in AML cells, we used granulocyte colony-stimulating factor (G-CSF) as a stimulus. G-CSF regulates the differentiation and function of neutrophils and has been employed in multiple studies investigating the involvement of STAT3 in myeloid differentiation [34, 35]. Since G-CSF stimulation leads to a robust increase in STAT3β phosphorylation after long-term treatment [35, 36], we used G-CSF for up to 10 days to provoke differentiation and STAT3 activation in *MLL-AF9* transformed FLCs. While all cells remained CD11b<sup>+</sup> (Fig. 2A), solely leukemia cells expressing both STAT3 isoforms responded to G-CSF by notable upregulation of the granulocytic surface marker Gr-1 (Fig. 2B), while on the mRNA level expression of the G-CSF receptor (*Csf3r*) was comparable in suspension culture (Fig. 2C). Furthermore, G-CSF stimulation did not lead to alterations in the expression of the hematopoietic stem cell (HSC)

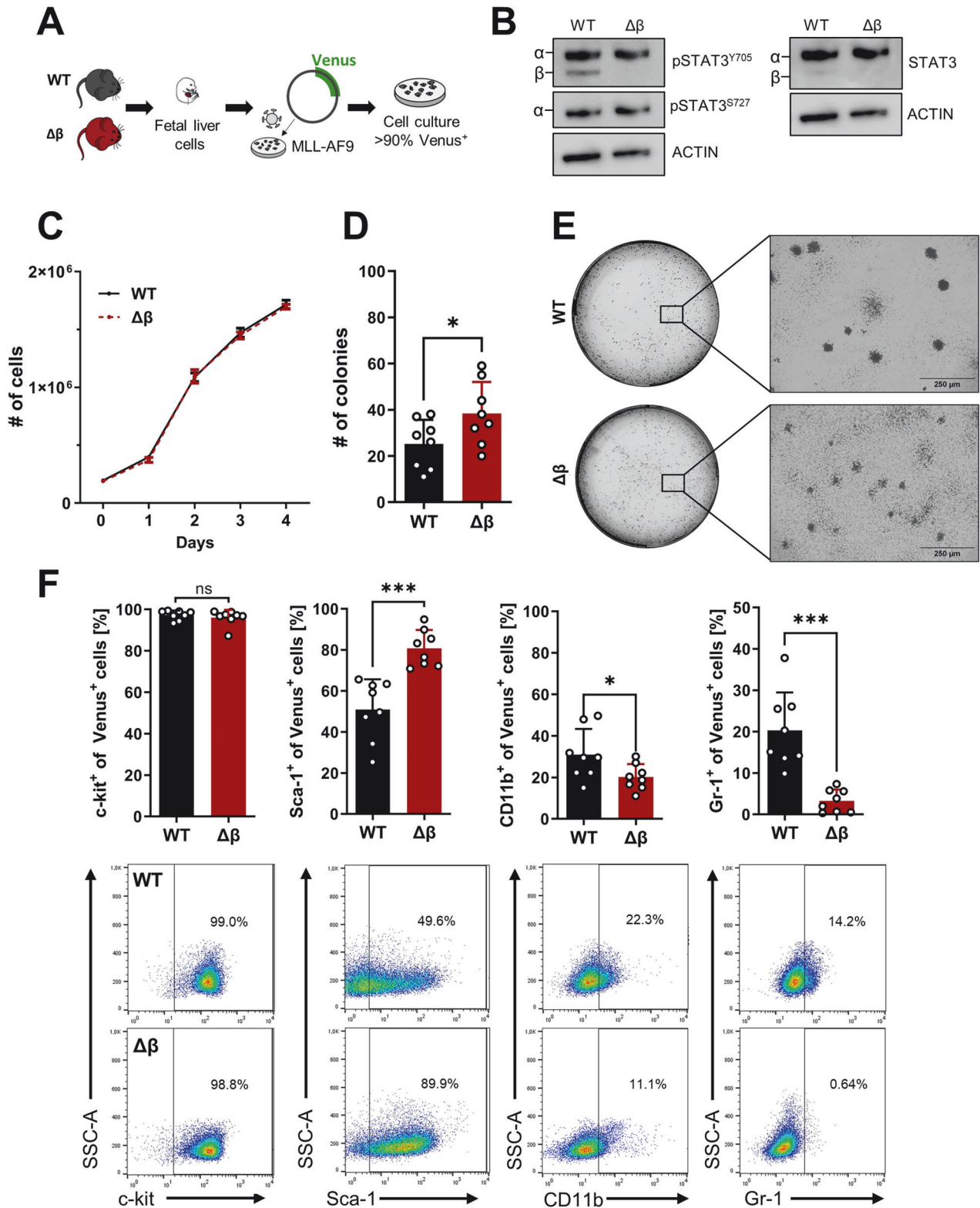


**Fig. 1** STAT3 $\beta$ -deficient leukemia cells display increased colony formation potential and are less committed to the myeloid lineage. **A** FLCs from WT and STAT3 $\beta$ -deficient ( $\Delta\beta$ ) mice were retrovirally transformed using a vector encoding *MLL-AF9*. **B** Western blot analysis of *MLL-AF9* transformed FLCs with the indicated antibodies. **C** Growth curves of *MLL-AF9* transformed FLCs ( $n = 6$ , 3 independent experiments, 2 cell lines). **D** Colony formation assay of WT and STAT3 $\beta$ -deficient leukemia cells ( $n = 8$ , 3 independent experiments with 3 serial replatings). **E** Representative pictures of colonies after 7 days in methylcellulose (40 $\times$  magnification). **F** Immunophenotyping of leukemia cells after 7 days in methylcellulose via flow cytometry and representative dot plots ( $n = 8$ , 3 experiments, 3 serial replatings). Statistical analysis was performed using Student's *t* test and indicated as  $p \leq 0.05$ :\*,  $\leq 0.01$ :\*\*. Error bars represent means  $\pm$  SD.

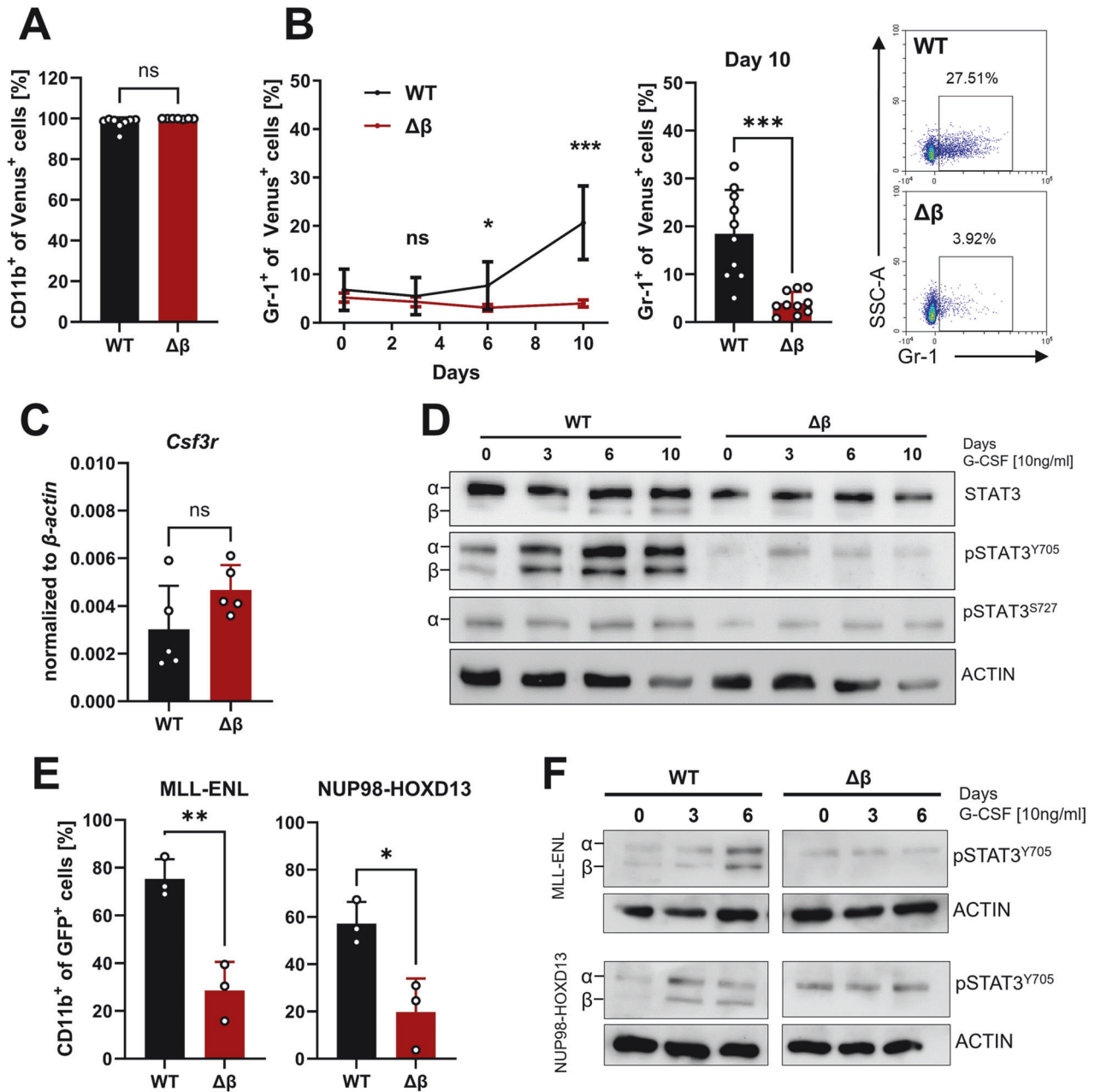


**Fig. 2** Leukemia cells lacking STAT3 $\beta$  exhibit reduced differentiation response to G-CSF. **A** Flow cytometry quantification of CD11b<sup>+</sup> cells after 10 days cultured with 10 ng/ml G-CSF. (n = 8, 3 independent experiments, 2–3 cell lines). **B** Quantification of Gr-1<sup>+</sup> cells after 10 days of G-CSF stimulation via flow cytometry and representative dot plots from day 10 (n = 10, 4 independent experiments, 2–3 cell lines). **C** RT-qPCR analysis of G-CSFR (*Csf3r*) expression in suspension culture (n = 5, 3 independent experiments, 2 cell lines). **D** Western blot of G-CSF stimulated samples with the indicated antibodies and time points. **E** Immunophenotyping of *MLL-ENL* and *NUP98-HOXD13* transformed FLCs after 10 days G-CSF via flow cytometry (n = 3, independent experiments). **F** Western blot of G-CSF stimulated samples (*MLL-ENL* and *NUP98-HOXD13* transformed FLCs) with the indicated antibodies and time points. Statistical analysis was performed using Student's *t* test and indicated as  $p \leq 0.05$ \*,  $\leq 0.01$ \*\*\*,  $\leq 0.001$ \*\*\*. Error bars represent means  $\pm$  SD.

markers c-kit and Sca-1 (Supplementary Fig. 2A). Three days of G-CSF stimulation resulted in a significant increase of STAT3 Y705 phosphorylation only in WT leukemia cells (Fig. 2D, Supplementary Fig. 2B). In contrast, serine 727 (S727) phosphorylation (Fig. 2D) and proliferation were not affected (Supplementary Fig. 2C). This phenomenon is not exclusive to *MLL-AF9* transformed FLCs but was also observed in two additional leukemia models, driven by the fusion genes *MLL-ENL* or *NUP98-HOXD13* [37, 38]. As on these cells Gr-1 was neither detected in suspension culture nor upon stimulation, we used the myeloid marker CD11b as a

readout. Upon G-CSF stimulation we detected increased CD11b expression (Fig. 2E) and strong phosphorylation of STAT3 Y705 (Fig. 2F) only when both STAT3 isoforms were present. Similar to our observations in *MLL-AF9*-driven leukemia cells, we did not observe a proliferation advantage in the absence of STAT3 $\beta$  in *MLL-ENL* or *NUP98-HOXD13*-driven leukemia cells (Supplementary Fig. 2D). Taken together, this data demonstrates that STAT3 $\beta$  plays—independent of the driver oncogene—a significant role in orchestrating myeloid differentiation in AML cells as its absence led to impaired myeloid differentiation in response to G-CSF.

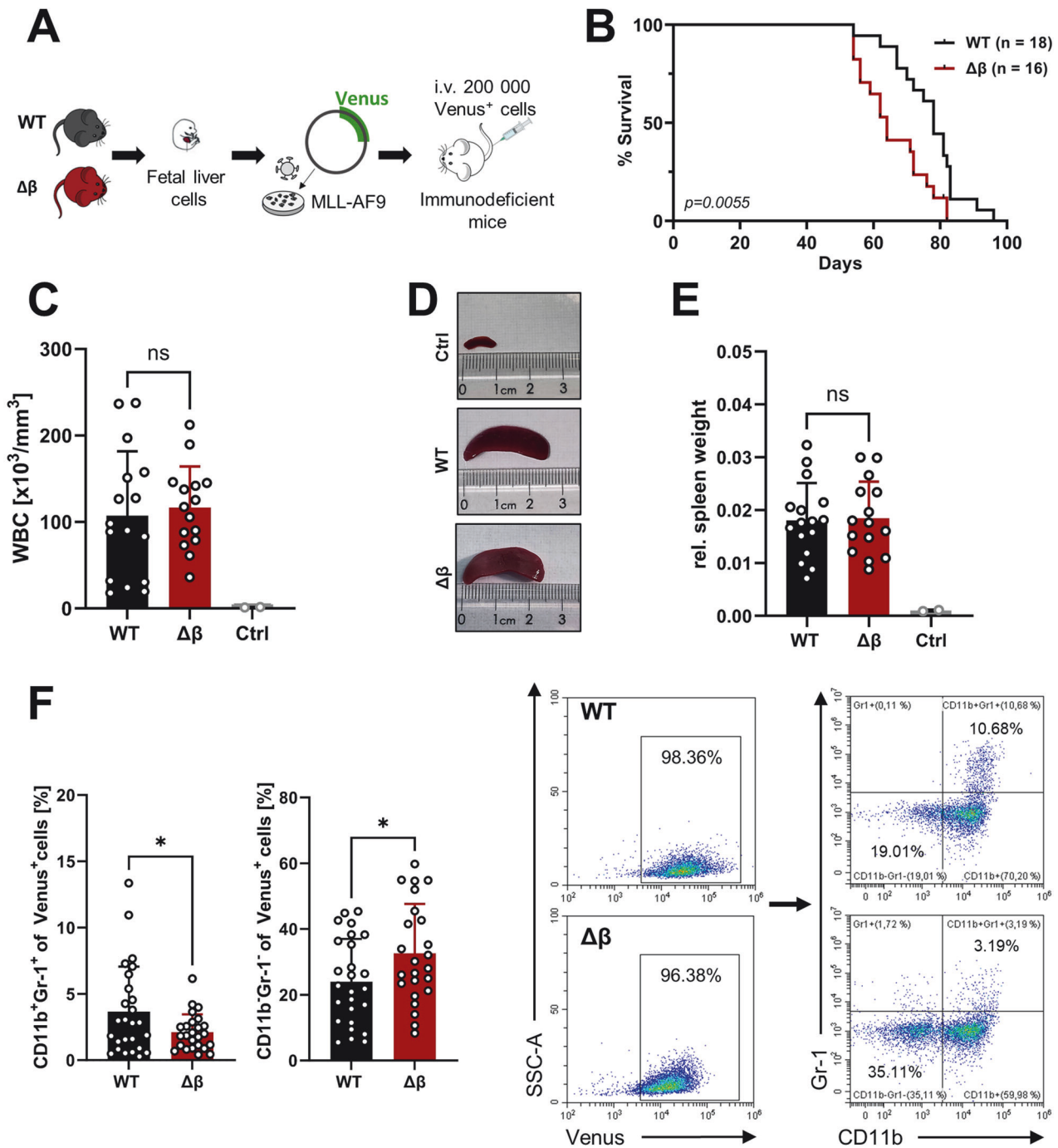


**Fig. 3 Absence of STAT3 $\beta$  accelerates disease progression in an *MLL-AF9*-dependent mouse model.** **A** 200 000 Venus<sup>+</sup> cells were intravenously (i.v.) transplanted into immunocompromised NOD.Cg-Prkdc<sup>scid</sup>Il2rg<sup>tm1Wjl</sup>/SzJ (NSG) mice. **B** Kaplan-Meier plot of mice receiving STAT3 $\beta$ -deficient or WT leukemia cells (3 independent experiments, median survival: WT = 78 days;  $\Delta\beta$  = 64 days). Log-rank (Mantel-Cox) test was performed to analyze the survival difference between the two groups ( $P = 0.0055$ ). **C** WBC count of diseased animals at the time point of euthanasia ( $n = 15$ ). **D** Representative pictures of spleens from diseased animals. **E** Spleen-to-body weight of diseased animals ( $n = 15$ , ctrl:  $n = 2$ ). **F** Flow cytometry quantification of myeloid markers on leukemia cells isolated from the BM and SP of each animal ( $n = 24$ , BM and SP pooled from 12 animals) and representative dot plots. Further statistical analysis was performed using Student's *t* test and indicated as  $p \leq 0.05$  \*. Error bars represent means  $\pm$  SD. (WBC white blood cell).

#### Absence of STAT3 $\beta$ accelerates disease progression in an *MLL-AF9*-dependent mouse model

We next intravenously transplanted *MLL-AF9* transformed WT or STAT3 $\beta$ -deficient FLCs into immunocompromised NSG mice and monitored disease progression *via* white blood cell counts (Fig. 3A, Supplementary Fig. 3A). Animals transplanted with STAT3 $\beta$ -deficient leukemia cells exhibited significantly shorter

OS (Fig. 3B) compared to mice receiving WT leukemia cells demonstrating its pivotal role as a tumor suppressor. At the endpoint no significant differences were observed between recipients of *MLL-AF9* transformed WT or STAT3 $\beta$ -deficient mice in leukemia infiltration of the bone marrow (BM) and spleen (SP) (Supplementary Fig. 3B), blasts detected in the peripheral blood (Fig. 3C, Supplementary Fig. 3C), spleen size (Fig. 3D), or ex vivo

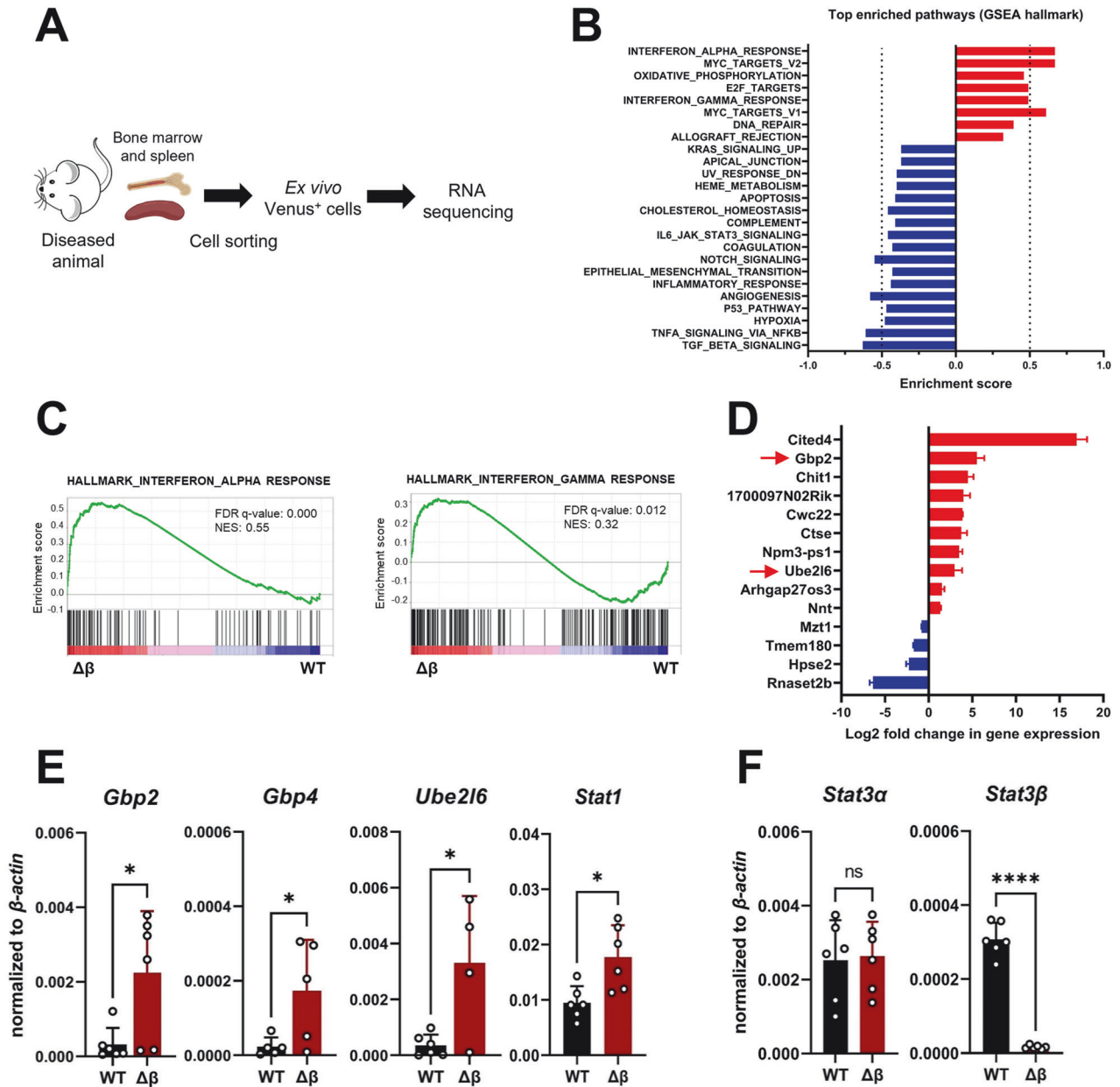


**Fig. 4 Gene expression analysis reveals enrichment of IFN-regulated genes in blasts lacking STAT3 $\beta$  isolated from diseased animals.** **A** Sample preparation for RNA sequencing (n = 3 per group and organ). For sorting strategy see Supplementary Fig. 4B. **B** Top enriched pathways (nominal p < 1%) in blasts lacking STAT3 $\beta$ . **C** GSEA plots of WT and STAT3 $\beta$ -deficient blasts isolated from SP of diseased animals (FDR False discovery rate, NES normalized enrichment score). **D** Significant hits shared between BM- and SP-derived blasts (n = 6). **E** RT-qPCR of ex vivo samples (n = 6, pooled BM and SP). **F** RT-qPCR on *Stat3* isoform expression in ex vivo samples from BM and SP (n = 6, pooled). Statistical analysis was performed using Student's *t* test and indicated as p < 0.05:\*, < 0.01:\*\*, < 0.001:\*\*\* and < 0.0001:\*\*\*\*. Error bars represent means  $\pm$  SD.

proliferation (Supplementary Fig. 3D). In contrast, and consistent with our in vitro data, blasts lacking STAT3 $\beta$  were less committed to the myeloid lineage (CD11b<sup>+</sup> Gr-1<sup>+</sup>) and comprise more CD11b<sup>+</sup>Gr-1<sup>-</sup> cells suggesting a more immature state in blasts lacking STAT3 $\beta$  (Fig. 3F). Together, these data indicate that the absence of STAT3 $\beta$  in blasts accelerates AML development and restricts myeloid differentiation in vivo, underscoring its role as a tumor suppressor.

#### Gene expression analysis reveals enrichment of IFN-regulated genes in blasts lacking STAT3 $\beta$

To identify STAT3 $\beta$ -regulated processes or target genes that affect disease outcome, blasts were isolated from the BM and SP

of diseased animals, sorted based on the co-expressed fluorophore Venus, and subjected to RNA sequencing (Fig. 4A, Supplementary Fig. 4A, B). To assess which cellular processes are dysregulated due to STAT3 $\beta$ -deficiency, we performed gene set enrichment analysis (GSEA). An enrichment of genes involved in IFN response, Myc targets, and oxidative phosphorylation was observed in the absence of STAT3 $\beta$  (Fig. 4B). In line with previous reports [2, 10], pathways related to hypoxia, inflammatory response, and IL6-JAK-STAT3 signaling were reduced in STAT3 $\beta$ -deficient blasts (Fig. 4B, Supplementary Fig. 4C). KEGG pathway analysis revealed that genes that were differentially expressed in the absence of STAT3 $\beta$  were enriched in the processes "hematopoietic cell lineage" and "cytokine-receptor

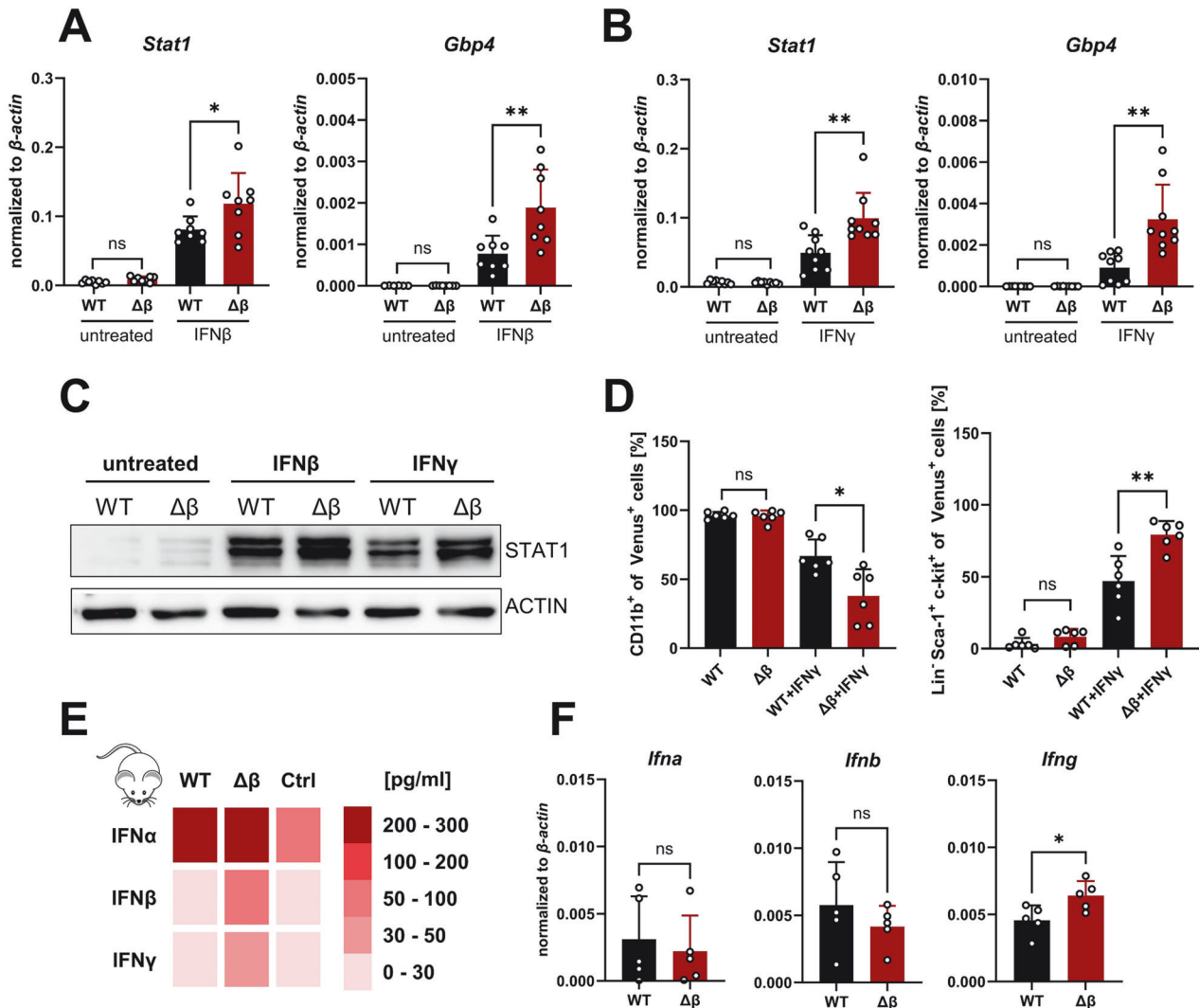


**Fig. 5** **STAT3 $\beta$  deficiency increases IFN responsiveness.** **A** mRNA expression after 3 h 100 U/ml IFN $\beta$  stimulation (n = 8, 3 independent experiments, 2–3 cell lines). **B** mRNA expression after 3 h 100 ng/ml IFN $\gamma$  stimulation (n = 9, 3 independent experiments, 3 cell lines). **C** Western blot after 24 h IFN treatment. **D** Flow cytometry quantification of CD11b<sup>+</sup> and Sca-1<sup>+</sup> cells after 48 h IFN $\gamma$  treatment (n = 6, 3 independent experiments, 2 cell lines). **E** Heatmap represents the average concentration measured in the plasma of diseased animals via multiplex assay. (n = 5 per group, 3 controls). **F** mRNA expression of *Ifna*, *Ifnb*, and *Ifng* in leukemia cells after 7 days in methylcellulose analyzed via RT-qPCR (n = 5, 3 independent experiments, 2 cell lines). Statistical analysis was performed using Student's *t* test and indicated as p  $\leq$  0.05; \*,  $\leq$  0.01; \*\*. Error bars represent means  $\pm$  SD.

interaction" (Supplementary Fig. 4D). This is in accordance with the observation that loss of STAT3 $\beta$  reduces myeloid differentiation of leukemia cells both in vitro and in vivo (Figs. 1F, 3F). GSEA revealed that a strong enrichment in gene expression in STAT3 $\beta$ -deficient blasts was observed in genes involved in type I (IFN $\alpha/\beta$ ) and type II (IFN $\gamma$ ) IFN signaling (Fig. 4C). By overlapping the significantly up- and downregulated genes between BM- and SP-derived blasts, we found *Gbp2* and *Ube2l6*, which are directly involved in IFN signaling, upregulated in the absence of STAT3 $\beta$  (Fig. 4D). Additionally, *Gbp4* and *Stat1* were among the highest upregulated genes in GSEA data (Supplementary Fig. 4E). RT-qPCR confirmed a threefold increase in *Ube2l6* and *Gbp2* expression and a twofold increase in *Stat1* expression, in STAT3 $\beta$ -deficient blasts (Fig. 4E). Moreover, *Stat3a* expression was comparable between blasts isolated from BM and SP confirming that the observed changes in gene expression are attributed to STAT3 $\beta$  rather than STAT3 $\alpha$  (Fig. 4F). Taken together, this data suggests that STAT3 $\beta$  represses IFN response in AML cells.

### STAT3 $\beta$ deficiency increases IFN responsiveness

To investigate whether the IFN response depends on STAT3 isoform expression, we stimulated *MLL-AF9* transformed FLCs for 3 h with either IFN $\beta$  or IFN $\gamma$ . While no differences occurred in the naive state, both agents caused a significantly stronger increase in the expression of IFN-inducible genes (*Gbp4*, *Stat1*) in STAT3 $\beta$ -deficient compared to WT leukemia cells (Fig. 5A, B). These differences were not caused by altered levels of interferon alpha/beta receptor 1 (IFNAR1) expression between genotypes (Supplementary Fig. 5A). After a 24 h stimulation with either IFN $\beta$  or IFN $\gamma$ , we observed increased levels of STAT1 protein in both genotypes. Interestingly, a higher expression was observed when STAT3 $\beta$  was absent (Fig. 5C, Supplementary Fig. 5B). In healthy HSCs, IFN $\gamma$  was shown to modulate lineage-specific myeloid differentiation [39] and to promote the expansion of Lin<sup>-</sup>Sca-1<sup>+</sup>c-kit<sup>+</sup> (LSK) cells potentially through upregulation of Sca-1 via JAK/STAT signaling [40, 41]. To assess the potential impact of IFN $\gamma$  on the differentiation state of AML cells, we treated the cells for 48 h with IFN $\gamma$  followed by immunophenotyping. Strikingly and in

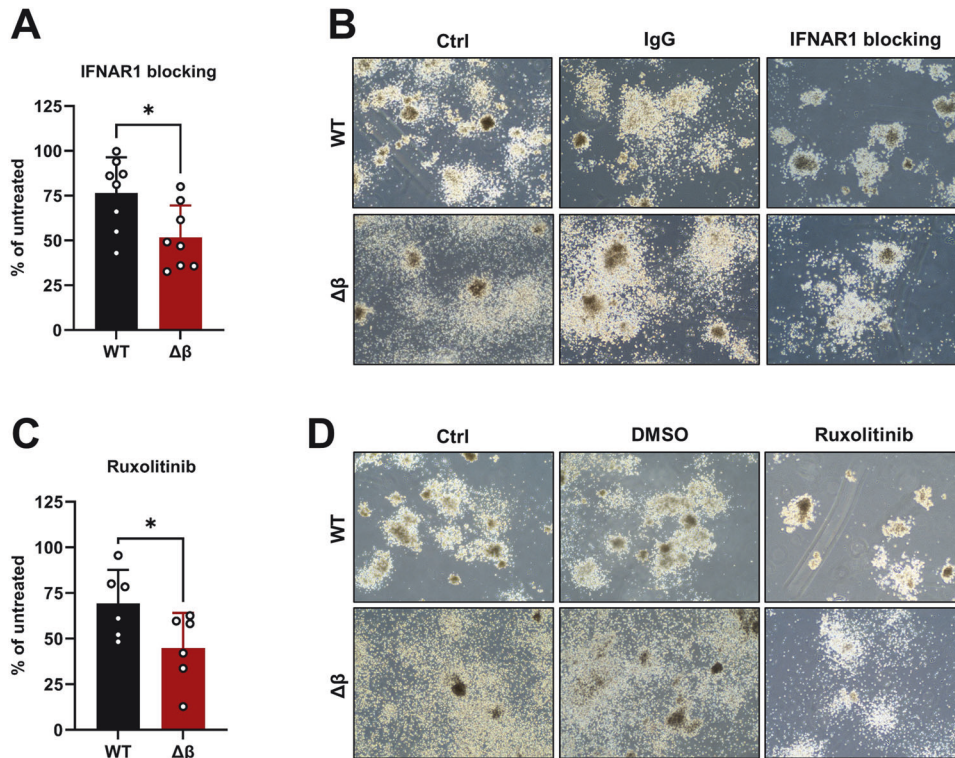


**Fig. 6 Interference with IFN signaling is a vulnerability of STAT3 $\beta$ -deficient cells.** **A** Colonies formed in the presence of 2  $\mu$ g/ml IFNAR1 blocking antibody normalized to untreated ( $n = 8$  from 3 independent experiments, 3 cell lines). **B** Representative images of colonies formed after 7 days in methylcellulose  $\pm$  IFNAR1 blocking antibody or IgG control. **C** Colonies formed in the presence of 5  $\mu$ M Ruxolitinib normalized to untreated ( $n = 6$ , 3 independent experiments, 2 cell lines). **D** Representative images of colonies formed  $\pm$  Ruxolitinib or DMSO control. Statistical analysis was performed using Student's  $t$  test and indicated as  $p \leq 0.05$ :\*. Error bars represent means  $\pm$  SD.

line with STAT3 $\beta$ -deficient leukemia cells displaying attenuated commitment to the myeloid lineage, a significant decrease in CD11b expression and an increase of LSK blasts was detected upon IFN $\gamma$  stimulation, which was stronger in leukemia cells lacking STAT3 $\beta$  (Fig. 5D, Supplementary Fig. 5C). These differences were independent of effects on cell viability (Supplementary Fig. 5D).

To investigate whether increased expression of IFN-inducible genes is linked to elevated cytokine production, we analyzed IFN levels in the plasma of leukemic mice. Remarkably, elevated levels of IFN $\alpha$ , IFN $\beta$ , and IFN $\gamma$  were detected in comparison to healthy controls (Fig. 5E). While high IFN $\alpha$  concentrations were found in both groups, we observed higher IFN $\beta$  and IFN $\gamma$  levels in the absence of STAT3 $\beta$ . In line with previous work demonstrating AML blasts themselves are capable of releasing IFN $\gamma$ , associated with poorer OS [42], we detected *Ifna*, *Ifnb* and *Ifng* expression after 7 days in methylcellulose, with a significantly higher *Ifng* expression in colonies formed by STAT3 $\beta$ -deficient leukemia cells (Fig. 5F). In summary, these data indicate that loss of STAT3 $\beta$  leads to enhanced IFN signaling, and potentially increased IFN production in leukemia cells.

#### Interference with IFN signaling is a vulnerability of STAT3 $\beta$ -deficient leukemia cells

Thus far, our data indicated that STAT3 $\beta$ -deficient leukemia cells induced disease at a significantly accelerated rate compared to WT cells (Fig. 3B), accompanied by enhanced IFN signaling (Fig. 4C). This suggests that increased expression of IFN-inducible genes may contribute to an adverse disease outcome. As we detected significantly higher IFN levels in the plasma of leukemic mice (Fig. 5E) and IFN-inducible genes in colonies, particularly in the absence of STAT3 $\beta$  (Supplementary Fig. 6A), we hypothesized that IFN signaling might contribute to the leukemogenic potential

of AML blasts. To assess whether interference with type I IFN signaling could ameliorate disease outcomes, we conducted colony formation assays (CFAs) in the presence and absence of an IFNAR1-blocking antibody. Indeed, we observed a substantial reduction of colony numbers after 7 days in methylcellulose for both WT and STAT3 $\beta$ -lacking leukemia cells with a stronger impact on the latter (Fig. 6A, B, Supplementary Fig. 6B, D). Accordingly, IFNAR1 blocking reduced IFN-inducible genes (*Stat1*, *Gbp4*, *Ube2l6*), in both groups (Supplementary Fig. 6C). To inhibit both type I and type II IFN signaling, we tested the JAK1/2 inhibitor Ruxolitinib. As expected, treatment with Ruxolitinib was sufficient to completely inhibit IFN $\gamma$ -induced upregulation of *Stat1* and *Gbp2* in *MLL-AF9* transformed FLCs (Supplementary Fig. 6E). Furthermore, Ruxolitinib treatment resulted in a significant reduction in colony numbers of STAT3 $\beta$ -deficient leukemia cells compared to WT cells (Fig. 6C, D, Supplementary Fig. 6F). To conclude, this data suggests that blockade of IFN signaling is a STAT3 $\beta$ -isoform specific vulnerability of leukemia cells, which could be of therapeutic relevance.

#### High expression of STAT1/IFN-inducible genes is associated with low STAT3 $\beta$ expression and with adverse outcomes in patients with AML

As our results indicate a link between IFN signaling and disease outcome, we explored the relevance of these findings in the clinical context. To validate the association between high expression of IFN-inducible genes and imbalanced STAT1/3 signaling, we accessed a patient cohort comprising 79 newly diagnosed AML patients (Supplementary Table 1). In line with our previous study, we confirmed in this new cohort *via* RT-qPCR that a low STAT3 $\beta/\alpha$  mRNA ratio correlates with adverse disease outcomes (Fig. 7A) which is independent of age and gender of the patients (Supplementary Fig. 7A, B). Notably, STAT3 $\beta$  levels



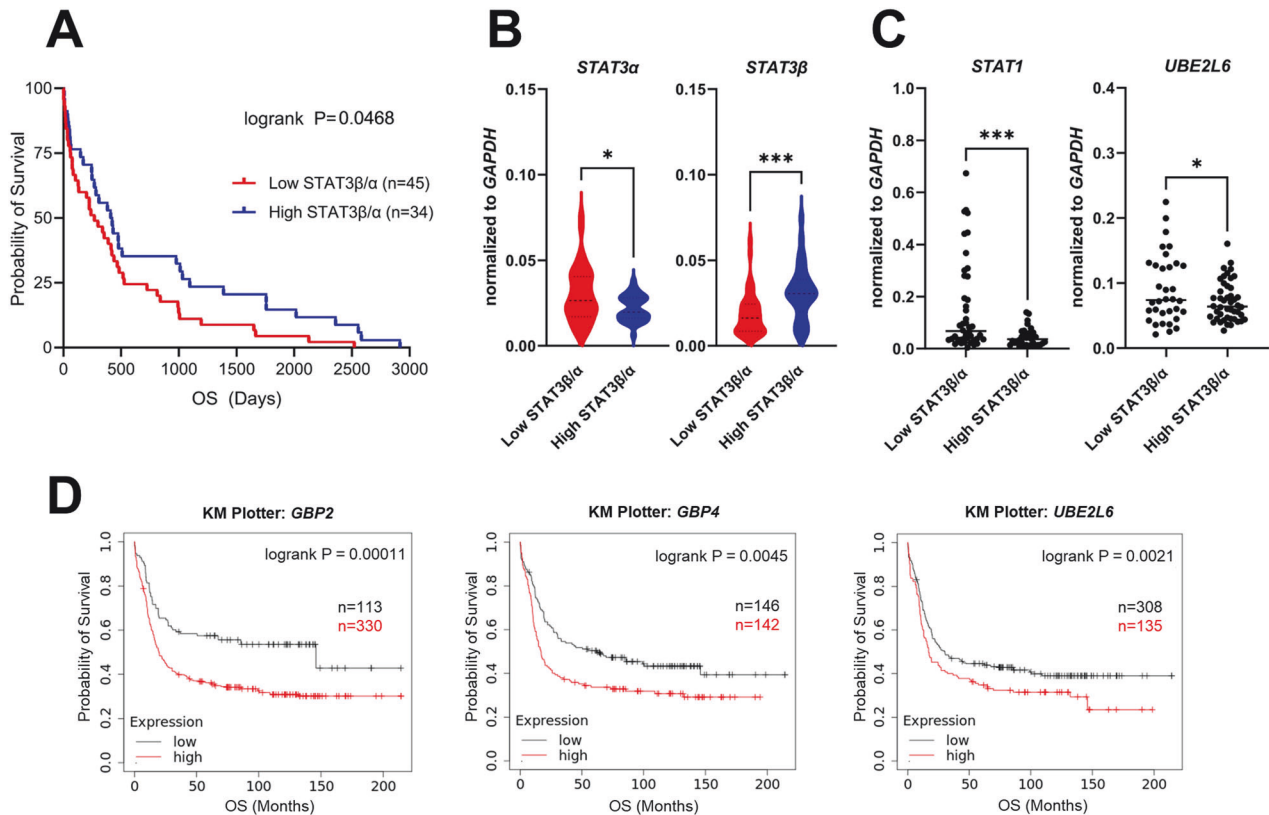


**Fig. 7 High expression of STAT1/IFN-inducible genes is associated with low *STAT3β* expression and adverse outcomes in AML patients.** **A** RT-qPCR analysis of *STAT3* isoform expression in 79 AML patient samples. A low *STAT3β/α* mRNA ratio correlates with poor OS. Patients were stratified according to the best cut-off value. Statistical analysis was performed using log-rank (Mantel-Cox) test. **B** RT-qPCR of *STAT3α* and *STAT3β* (normalized to *GAPDH*) in patients with a low or high *STAT3β/α* ratio ( $n = 79$ ). Data were compared using the Student's *t* test. **C** *STAT1* and *UBE2L6* expression in patients with a low or high *STAT3β/α* ratio ( $n = 79$ ). Data were compared using the Student's *t* test. **D** KM Plotter analysis of RNA sequencing data of AML patients showing a correlation between high expression of *GBP2*, *GBP4*, and *UBE2L6* with OS. Patients were stratified according to the best cut-off value. (kmplot.com), status: 15.01.2024. Statistical analysis was performed using log-rank (Mantel-Cox) test.  $p \leq 0.05$ .\*;  $\leq 0.01$ .\*\*;  $\leq 0.001$ \*\*\*.

were primarily responsible for a lower *STAT3β/α* ratio, while *STAT3α* expression appears to be of less relevance (Fig. 7B). Intriguingly, patients with low *STAT3β/α* ratio displayed a significantly higher *STAT1* and *UBE2L6* gene expression (Fig. 7C). In this cohort we noted a trend suggesting higher expression of *STAT1* and IFN-inducible genes is potentially associated with adverse disease outcomes (Supplementary Fig. 7C). We therefore tested this in a larger patient cohort using two different publicly available RNA sequencing data sets of AML patients (KM Plotter: Affymetrix, BloodSpot: TCGA), and correlated the expression of IFN-inducible genes to OS. Remarkably, high expression of *GBP2* and *UBE2L6* correlated with significantly poorer OS in both cohorts (Fig. 7D, Supplementary Fig. 7D). To conclude, we here describe a specific contribution of *STAT3β* in fine-tuning IFN response by repressing *STAT1*-mediated IFN signaling in AML blasts, which improves disease outcome.

## DISCUSSION

We previously demonstrated that the *STAT3β/α* mRNA ratio serves as a prognostic marker, correlating with disease outcomes in AML patients [19]. Here, we provide strong evidence for *STAT3β* acting as a tumor suppressor in AML and uncovered the underlying mechanism behind its protective role. The absence of *STAT3β* in AML cells led to impaired G-CSF-induced myeloid differentiation and *STAT3α* phosphorylation *in vitro*. Using an *MLL-AF9*-driven AML mouse model we confirmed a reduced commitment to the myeloid lineage in leukemia cells *in vivo*. The imbalance of *STAT3*

isoforms in leukemia cells resulted in enhanced IFN signaling in the absence of *STAT3β* together with shorter survival of leukemic mice. Intriguingly, we confirmed that higher expression of IFN-inducible genes correlates with shorter OS in AML patients.

The impact of *STAT3* on regulating the balance between self-renewal and differentiation of HSCs is highly dependent on the type of hematopoietic progenitor and the stimulus. Especially during myeloid differentiation in response to G-CSF, robust and sustained *STAT3* activation is crucial for differentiation and survival of myeloid progenitors [43–45]. Several studies reported increased *STAT3β* activity upon G-CSF-induced myeloid differentiation in healthy but also transformed leukemia cells [34, 35]. Accordingly, phosphorylation of *STAT3* in response to G-CSF in murine leukemia cells only occurred if both isoforms were present. Interestingly, phosphorylation of *STAT3α* in *STAT3β*-deficient blasts also remained absent, together with impaired myeloid differentiation. These findings indicate that *STAT3β* is pivotal for a G-CSF-induced myeloid differentiation program in AML blasts. As we did not observe alterations in G-CSF receptor (*Csf3r*) mRNA expression or in proliferation upon G-CSF stimulation, we assume that the absence of *STAT3β* does not affect receptor expression *per se*, but rather impairs endosomal recycling of the receptor causing reduced signaling, as previously suggested [46–48]. However, to obtain more detailed mechanistic insights further research is required. *In vivo*, we also identified a reduction in myeloid lineage commitment in blasts lacking *STAT3β*, together with more rapid disease progression. Consistent with this, pediatric AML patient samples with low *STAT3* phosphorylation

upon G-CSF stimulation showed poorer OS than patients with a stronger STAT3 response [46].

As anticipated, the absence of STAT3 $\beta$  led to accelerated disease progression, together with enhanced IFN signaling *in vivo*. Since IFN signaling plays a central role in cancer progression by promoting inflammation and reprogramming the tumor microenvironment, but also in multiple anti-tumor properties, its effects are highly context-dependent [49–51]. In AML patients, IFN signatures have been reported to correlate with favorable prognosis [52, 53], and negative outcomes as well [42]. One possible explanation for these contradictory results could be a concentration-dependent effect of IFN leading to either an acute or chronic response [51, 54]. While we observed high IFN $\alpha$  concentrations in the plasma of diseased animals in both groups, we detected IFN $\beta$  and IFN $\gamma$  to a higher extent in the absence of STAT3 $\beta$ . Constant production of IFN at a low level, also known as tonic signaling [55], was reported for AML blasts leading to rearrangement of the tumor microenvironment driving leukemogenesis [42]. Accordingly, we observed that blocking type I IFN signaling leads to impaired colony formation ability, particularly in the absence of STAT3 $\beta$ . Furthermore, interference with both type I and type II IFN signaling with Ruxolitinib resulted in significantly decreased colony formation of STAT3 $\beta$ -deficient blasts. Ruxolitinib, approved for myeloproliferative neoplasms, was tested in clinical trials including patients with secondary AML or relapsed patients with moderate effectiveness [56].

Since STAT1 expression was elevated in STAT3 $\beta$ -deficient leukemia cells along with IFN-inducible genes, we postulate that the enhanced IFN signaling results from an imbalance in STAT1/3 signaling due to the absence of STAT3 $\beta$ . While STAT1 and STAT3 activate transcription of an overlapping set of genes, they do not bind to identical DNA elements, which is likely to account for their distinct biological effects [57]. In line, the balance between STAT1/STAT3 activation in response to IFN determines the inflammatory potency in healthy but also transformed cells [58, 59]. IFN $\beta$  and IFN $\gamma$  stimulation in the absence of STAT3 $\beta$  *in vitro* revealed significantly higher expression of STAT1 as well as other IFN-inducible genes. In accordance, STAT3 has been described to attenuate STAT1-mediated IFN signaling [58, 59]. However, in our setting, loss of STAT3 $\beta$  alone was sufficient to enhance STAT1 expression in AML blasts. To ascertain the clinical relevance, we analyzed 79 AML patient samples. *STAT1* and the IFN-inducible gene *UBE2L6* were significantly higher expressed in patients with a low *STAT3 $\beta$ / $\alpha$*  mRNA ratio. Using two distinct publicly available RNA sequencing data sets of AML patients, we confirmed a correlation between higher expression of a set of IFN-inducible genes with poorer OS.

To conclude, in this study, we gained novel insights into the protective role of STAT3 $\beta$  in AML. STAT3 $\beta$  favors myeloid differentiation and fine-tunes tonic IFN signaling in experimental mice and human AML patients. We here describe for the first time STAT3 $\beta$  as a repressor of IFN signaling in AML blasts by maintaining the balance of STAT1-mediated IFN signaling. Thus, using the *STAT3 $\beta$ / $\alpha$*  mRNA ratio as a prognostic marker could hold crucial information for targeted treatment approaches. Specifically, patients exhibiting a low *STAT3 $\beta$ / $\alpha$*  ratio could benefit from therapeutic interventions targeting STAT1/IFN signaling.

## DATA AVAILABILITY

RNA sequencing data is available via Gene Expression Omnibus (GEO) database under accession number GSE261198.

## REFERENCES

1. Cancer SEER Statistics Review (CSR) 1975–2017. 2024: [https://seer.cancer.gov/archive/csr/1975\\_2017/](https://seer.cancer.gov/archive/csr/1975_2017/).
2. Levy DE, Lee C. What does Stat3 do? *J Clin Invest*. 2002;109:1143–114.
3. Huynh J, Chand A, Gough D, Ernst M. Therapeutically exploiting STAT3 activity in cancer—using tissue repair as a road map. *Nat Rev Cancer*. 2018;19:82–96.
4. Benekli M, Xia Z, Donohue KA, Ford LA, Pixley LA, Baer MR, et al. Constitutive activity of signal transducer and activator of transcription 3 protein in acute myeloid leukemia blasts is associated with short disease-free survival. *Blood*. 2002;99:252–7.
5. Zhou J, Bi C, Janakakumara JV, Liu SC, Chng WJ, Tay KG, et al. Enhanced activation of STAT pathways and overexpression of survivin confer resistance to FLT3 inhibitors and could be therapeutic targets in AML. *Blood*. 2009;113:4052–62.
6. Steensma DP, McClure RF, Karp JE, Tefferi A, Lasho TL, Powell HL, et al. JAK2 V617F is a rare finding in de novo acute myeloid leukemia, but STAT3 activation is common and remains unexplained. *Leukemia*. 2006;20:971–8.
7. Gouilleux-Gruart V, Gouilleux F, Desaint C, Claisse J, Capiod J, Delobel J, et al. STAT-related transcription factors are constitutively activated in peripheral blood cells from acute leukemia patients. *Blood*. 1996;87:1692–7.
8. Redell MS, Ruiz MJ, Alonzo TA, Gerbing RB, Tweardy DJ. Stat3 signaling in acute myeloid leukemia: ligand-dependent and -independent activation and induction of apoptosis by a novel small-molecule Stat3 inhibitor. *Blood*. 2011;117:5701–9.
9. Schuringa JJ, Wierenga ATJ, Kruijer W, Vellenga E. Constitutive Stat3, Tyr705, and Ser727 phosphorylation in acute myeloid leukemia cells caused by the autocrine secretion of interleukin-6. *Blood*. 2000;95:3765–70.
10. Aigner P, Just V, Stoiber D. STAT3 isoforms: alternative fates in cancer? *Cytokine*. 2018;118:27–34.
11. Maritano D, Sugrue ML, Tinini S, Dewilde S, Strobl B, Fu X, et al. The STAT3 isoforms  $\alpha$  and  $\beta$  have unique and specific functions. *Nat Immunol*. 2004;5:401–9.
12. Dewilde S, Vercelli A, Chiarle R, Poli V. Of alphas and betas: distinct and overlapping functions of STAT3 isoforms. *Front Biosci*. 2008;13:6501–14.
13. Shao H, Quintero AJ, Tweardy DJ. Identification and characterization of cis elements in the STAT3 gene regulating STAT3 $\alpha$  and STAT3 $\beta$  messenger RNA splicing. *Blood*. 2011;98:3853–6.
14. Caldenhoven E, Van Dijk TB, Solari R, Armstrong J, Raaijmakers JAM, Lammers JWJ, et al. STAT3 $\beta$ , a splice variant of transcription factor STAT3, is a dominant negative regulator of transcription. *J Biol Chem*. 1996;271:13221–7.
15. Ng IHW, Ng DCH, Jans DA, Bogoyevitch MA. Selective STAT3- $\alpha$  or - $\beta$  expression reveals spliceform-specific phosphorylation kinetics, nuclear retention and distinct gene expression outcomes. *Biochem J*. 2012;447:125–36.
16. Zhang HF, Chen Y, Wu C, Wu ZY, Tweardy DJ, Alshareef A, et al. The opposing function of STAT3 as an oncoprotein and tumor suppressor is dictated by the expression status of STAT3 $\beta$  in esophageal squamous cell carcinoma. *Clin Cancer Res*. 2016;22:691–703.
17. Ivanov VN, Zhou H, Partridge MA, Hei TK. Inhibition of ataxia telangiectasia mutated kinase activity enhances TRAIL-mediated apoptosis in human melanoma cells. *Cancer Res*. 2009;69:3510–9.
18. Xu G, Zhang C, Zhang J. Dominant negative STAT3 suppresses the growth and invasion capability of human lung cancer cells. *Mol Med Rep*. 2009;2:819–24.
19. Aigner P, Mizutani T, Horvath J, Eder T, Heber S, Lind K, et al. STAT3 $\beta$  is a tumor suppressor in acute myeloid leukemia. *Blood Adv*. 2019;3:1989–2002.
20. Lal R, Lind K, Heitzer E, Ulz P, Aubell K, Kashofer K, et al. Somatic TP53 mutations characterize preleukemic stem cells in acute myeloid leukemia. *Blood*. 2017;129:2587–91.
21. Döhner H, Wei AH, Appelbaum FR, Craddock C, DiNardo CD, Dombret H, et al. Diagnosis and management of AML in adults: 2022 recommendations from an international expert panel on behalf of the ELN. *Blood*. 2022;140:1345–77.
22. Yoshimoto G, Miyamoto T, Jabbarzadeh-Tabrizi S, Iino T, Rocnik JL, Kikushige Y, et al. FLT3-ITD up-regulates MCL-1 to promote survival of stem cells in acute myeloid leukemia via FLT3-ITD-specific STAT5 activation. *Blood*. 2009;114:5034–43.
23. Kotecha N, Flores NJ, Irish JM, Simonds EF, Sakai DS, Archambeault S, et al. Single-cell profiling identifies aberrant STAT5 activation in myeloid malignancies with specific clinical and biologic correlates. *Cancer Cell*. 2008;14:335–43.
24. Choudhary C, Müller-Tidow C, Berdel WE, Serve H. Signal transduction of oncogenic Flt3. *Int J Hematol*. 2005;82:93–99.
25. Mizuki M, Schwäbe J, Steur C, Choudhary C, Agrawal S, Sargin B, et al. Suppression of myeloid transcription factors and induction of STAT response genes by AML-specific Flt3 mutations. *Blood*. 2003;101:3164–73.
26. Spiekermann K, Bagrintseva K, Schwab R, Schmieja K, Hiddemann W. Overexpression and constitutive activation of FLT3 induces STAT5 activation in primary acute myeloid leukemia blast cells. *Clin Cancer Res*. 2003;9:2140–50.
27. Lániczky A, Györfy B. Web-based survival analysis tool tailored for medical research (KMplot): development and implementation. *J Med Internet Res*. 2021;23:e27633.
28. Bagger FO, Sasivarevic D, Sohi SH, Laursen LG, Pundhir S, Sønderby CK, et al. BloodSpot: a database of gene expression profiles and transcriptional programs for healthy and malignant haematopoiesis. *Nucleic Acids Res*. 2016;44:917–24.
29. Nagy Á, Munkácsy G, Györfy B. Pancancer survival analysis of cancer hallmark genes. *Sci Rep*. 2021;11:6047.

30. Matsuo Y, MacLeod RAF, Uphoff CC, Drexler HG, Nishizaki C, Katayama Y, et al. Two acute monocytic leukemia (AML-M5a) cell lines (MOLM-13 and MOLM-14) with interclonal phenotypic heterogeneity showing MLL-AF9 fusion resulting from an occult chromosome insertion, *ins(11;9)(q23;p22p23)*. *Leukemia*. 1997;11:1469–77.
31. Stubbs MC, Krivtsov AV. Murine retrovirally-transduced bone marrow engraftment models of MLL-fusion-driven acute myelogenous leukemias (AML). *Curr Protoc Pharmacol*. 2017;78:14.42.1–14.42.19.
32. Winters AC, Bernt KM. MLL-rearranged leukemias—an update on science and clinical approaches. *Front Pediatr*. 2017;5:240371.
33. Skucha A, Ebner J, Schmöllerl J, Roth M, Eder T, César-Razquin A, et al. MLL-fusion-driven leukemia requires SETD2 to safeguard genomic integrity. *Nat Commun*. 2018;9:1983.
34. Chakraborty A, White SM, Schaefer TS, Ball ED, Dyer KF, Tweardy DJ. Granulocyte colony-stimulating factor activation of Stat3 $\alpha$  and Stat3 $\beta$  in immature normal and leukemic human myeloid cells. *Blood*. 1996;88:2442–9.
35. Chakraborty A, Tweardy DJ. Stat3 and G-CSF-induced myeloid differentiation. *Leuk Lymphoma*. 1998;30:433–42.
36. Hevehan DL, Miller WM, Papoutsakis ET. Differential expression and phosphorylation of distinct STAT3 proteins during granulocytic differentiation. *Blood*. 2002;99:1627–37.
37. Bach C, Mueller D, Buhl S, Garcia-Cuellar MP, Slany RK. Alterations of the Cxcr domain preclude oncogenic activation of mixed-lineage leukemia 2. *Oncogene*. 2009;28:815–23.
38. Lin YW, Slape C, Zhang Z, Aplan PD. NUP98-HOXD13 transgenic mice develop a highly penetrant, severe myelodysplastic syndrome that progresses to acute leukemia. *Blood*. 2009;106:287.
39. King KY, Goodell MA. Inflammatory modulation of HSCs: viewing the HSC as a foundation for the immune response. *Nat Rev Immunol*. 2011;11:685–92.
40. Zhao X, Ren G, Liang L, Ai PZ, Zheng B, Tischfield JA, et al. Brief report: interferon-gamma induces expansion of Lin(-)Sca-1(+)-C-Kit(+) Cells. *Stem Cells*. 2010;28:122–6.
41. Snapper CM, Yamaguchi H, Urban JF, Finkelman FD. Induction of Ly-6A/E expression by murine lymphocytes after *in vivo* immunization is strictly dependent upon the action of IFN- $\alpha$ /beta and/or IFN- $\gamma$ . *Int Immunol*. 1991;3:845–52.
42. Corradi G, Bassani B, Simonetti G, Sangaletti S, Vadakekolathu J, Fontana MC, et al. Release of IFN $\gamma$  by acute myeloid leukemia cells remodels bone marrow immune microenvironment by inducing regulatory T cells. *Clin Cancer Res*. 2022;28:3141–55.
43. Shimozaki K, Nakajima K, Hirano T, Nagata S. Involvement of STAT3 in the granulocyte colony-stimulating factor-induced differentiation of myeloid cells. *J Biol Chem*. 1997;40:25184–9.
44. Ward AC, Smith L, De Koning JP, Van Aesch Y, Touw IP. Multiple signals mediate proliferation, differentiation, and survival from the granulocyte colony-stimulating factor receptor in myeloid 32D cells. *J Biol Chem*. 1999;93:113–24.
45. De Koning JP, Soede-Bobok AA, Ward AC, Schelen AM, Antonissen C, Van Leeuwen D, et al. STAT3-mediated differentiation and survival of myeloid cells in response to granulocyte colony-stimulating factor: role for the cyclin-dependent kinase inhibitor p27 Kip1. *Oncogene*. 2000;19:3290–8.
46. Narayanan P, Man TK, Gerbing RB, Ries R, Stevens AM, Wang YC, et al. Aberrantly low STAT3 and STAT5 responses are associated with poor outcome and an inflammatory gene expression signature in pediatric acute myeloid leukemia. *Clin Transl Oncol*. 2021;23:2141.
47. Carbone CJ, Fuchs SY. Elminative signaling by Janus kinases: role in the down-regulation of associated receptors. *J Cell Biochem*. 2014;115:8–16.
48. Schmid SL. Reciprocal regulation of signaling and endocytosis: Implications for the evolving cancer cell. *J Cell Biol*. 2017;216:2623–32.
49. Kollmann S, Grundschober E, Maurer B, Warsch W, Grausenburger R, Edlinger L, et al. Twins with different personalities: STAT5B-but not STAT5A-has a key role in BCR/ABL-induced leukemia. *Leukemia*. 2019;33:1583–97.
50. Ciciarello M, Corradi G, Sangaletti S, Bassani B, Simonetti G, Vadakekolathu J, et al. Interferon- $\gamma$ -dependent inflammatory signature in acute myeloid leukemia cells is able to shape stromal and immune bone marrow microenvironment. *Blood*. 2019;134:1212.
51. Parker BS, Rautela J, Hertzog PJ. Antitumor actions of interferons: implications for cancer therapy. *Nat Rev Cancer*. 2016;16:131–44.
52. Holicek P, Truxova I, Rakova J, Salek C, Hensler M, Kovar M, et al. Type I interferon signaling in malignant blasts contributes to treatment efficacy in AML patients. *Cell Death Dis*. 2023;14:209.
53. Curran E, Bell J, Venkataraman G, Fidai S, Godley L, Kline J. Type I interferon signaling predicts inferior survival in patients with AML. *Clin Lymphoma Myeloma Leuk*. 2019;19:S241.
54. Boukhaled GM, Harding S, Brooks DG. Opposing roles of type I interferons in cancer immunity. *Annu Rev Pathol*. 2021;16:167–98.
55. Gough DJ, Messina NL, Clarke CJP, Johnstone RW, Levy DE. Constitutive type I interferon modulates homeostatic balance through tonic signaling. *Immunity*. 2012;36:166–74.
56. Eghtedar A, Verstovsek S, Estrov Z, Burger J, Cortes J, Bivins C, et al. Phase 2 study of the JAK kinase inhibitor ruxolitinib in patients with refractory leukemias, including postmyeloproliferative neoplasm acute myeloid leukemia. *Blood*. 2012;119:4614–8.
57. Horvath CM, Wen Z, Darnell JE. A STAT protein domain that determines DNA sequence recognition suggests a novel DNA-binding domain. *Genes Dev*. 1995;9:984–94.
58. Ho HH, Ivashkiv LB. Role of STAT3 in type I interferon responses: negative regulation of STAT1-dependent inflammatory gene activation. *J Biol Chem*. 2008;281:14111–8.
59. Qing Y, Stark GR. Alternative activation of STAT1 and STAT3 in response to interferon- $\gamma$ . *J Biol Chem*. 2004;279:41679–85.

## ACKNOWLEDGEMENTS

The authors thank Johannes Zuber for the pMSCV-MLL-AF9-IRES-Venus construct. We thank Christoph Bock and the Biomedical Sequencing Facility of the Medical University of Vienna for help with RNA sequencing. We are grateful to Birgit Strobl, Karoline Kollmann, and Sebastian Kollmann for helpful discussions. We thank Petra Aigner and Tatsuaki Mizutani who provided expertise that assisted the research. Lastly, we would like to thank Jaqueline Horvath and all members of the animal facility for their support. This research was funded in whole or in part by the Austrian Science Fund (FWF, 10.55776/P32693 to DS, 10.55776/P36728, 10.55776/P33430, 10.55776/P32900 and 10.55776/DOCS9 to EC), City of Vienna Fund for Innovative, Interdisciplinary Cancer Research to EC, Italian Cancer Research Association (AIRC IG16930) to VP, and Gesellschaft für Forschungsförderung Niederösterreich m.b.H. (GFF, SC19-019 and LSC19-019) to DS. For open access purposes, the author has applied for a CC BY public copyright license to any Author Accepted Manuscript version arising from this submission. We also acknowledge support by Open Access Publishing Fund of Karl Landsteiner University of Health Sciences, Krems, Austria. BG was supported by the National Research, Development, and Innovation Office (PharmaLab, RRF-2.3.1-21-2022-00015). SE is a PhD candidate at the Medical University of Vienna. This work is submitted in partial fulfillment of the requirement for a PhD.

## AUTHOR CONTRIBUTIONS

SE, AW-S, BZ, and DS designed the research; SE, AW-S, KH, BZ, and SW performed experiments, analyzed, and interpreted data; BZ and TE performed bioinformatics analysis of RNA sequencing data; SD and HS provided AML patient samples and clinical information; UG and SK helped with statistical analysis; OS, RW, BG, VP, EC, and FG provided essential material and discussion. SE and DS wrote the manuscript. AW-S, BZ and DS revised the manuscript. The manuscript was approved by all authors.

## COMPETING INTERESTS

The authors declare no competing interests.

## ETHICS

Analysis of patient-derived samples was approved by the Scientific Integrity and Ethics Committee of the Karl Landsteiner University of Health Sciences (Austria) under license 1030/2023 and conducted according to the Declaration of Helsinki. All animal experiments were approved by the Animal Ethics Committee of the Medical University of Vienna and the Austrian Ministry of Education, Science and Research under license GZ BMBWF-66.009/0410-V/3b/2018 and performed according to the FELASA guidelines.

## ADDITIONAL INFORMATION

**Supplementary information** The online version contains supplementary material available at <https://doi.org/10.1038/s41419-024-06749-9>.

**Correspondence** and requests for materials should be addressed to Dagmar Stoiber.

**Reprints and permission information** is available at <http://www.nature.com/reprints>

**Publisher's note** Springer Nature remains neutral with regard to jurisdictional claims in published maps and institutional affiliations.



**Open Access** This article is licensed under a Creative Commons Attribution 4.0 International License, which permits use, sharing, adaptation, distribution and reproduction in any medium or format, as long as you give appropriate credit to the original author(s) and the source, provide a link to the Creative Commons licence, and indicate if changes were made. The images or other third party material in this article are included in the article's Creative Commons licence, unless indicated otherwise in a credit line to the material. If material is not included in the article's Creative Commons licence and your intended use is not permitted by statutory regulation or exceeds the permitted use, you will need to obtain permission directly from the copyright holder. To view a copy of this licence, visit <http://creativecommons.org/licenses/by/4.0/>.

© The Author(s) 2024